



# Comparison of computed tomography and magnetic resonance imaging findings and histopathological features of macrotrabecular-massive hepatocellular carcinoma

Qishu Gong, Yusen Zhang, Tianchong Wu, Zhiyong Du, Yue Zhang

Department of Hepatobiliary Surgery, Shenzhen People's Hospital (The Second Clinical Medical College, Jinan University; The First Affiliated Hospital, Southern University of Science and Technology), Shenzhen, China

*Contributions:* (I) Conception and design: Q Gong; (II) Administrative support: Yue Zhang; (III) Provision of study materials or patients: Yusen Zhang, T Wu, Z Du; (IV) Collection and assembly of data: Q Gong; (V) Data analysis and interpretation: Q Gong, Yue Zhang; (VI) Manuscript writing: All authors; (VII) Final approval of manuscript: All authors.

*Correspondence to:* Yue Zhang, PhD. Department of Hepatobiliary Surgery, Shenzhen People's Hospital (The Second Clinical Medical College, Jinan University; The First Affiliated Hospital, Southern University of Science and Technology), Dongmen Beilu 1017, Shenzhen 518020, China. Email: szrmyy@126.com.

**Background:** Macrotrabecular-massive hepatocellular carcinoma (MTM-HCC) is a novel subtype of HCC, one of eight distinct subtypes, that accounts for 5% of all cases of HCC and is associated with a worse prognosis. Preoperative diagnosis of MTM-HCCs using imaging findings can facilitate patient treatment decision-making. The purpose of this study was to describe computed tomography (CT) and magnetic resonance imaging (MRI) findings of MTM-HCCs and compare these findings with histopathological features.

**Methods:** This retrospective case-control study was performed at Shenzhen People's Hospital. The cohort included 17 patients with surgically confirmed MTM-HCCs and 232 patients with surgically confirmed non-MTM-HCCs who were enrolled by searching the pathological database from January 2018 to June 2022. CT and MRI findings were retrospectively analyzed and compared with pathological features. Student's *t*-test or Mann-Whitney U test for continuous variables and  $\chi^2$  test or Fisher's exact test for categorical variables were implemented to compare imaging manifestations between MTM-HCCs and non-MTM-HCCs, as appropriate.

**Results:** Seventeen tumors with a mean diameter of  $8.58 \pm 2.83$  cm were identified in the 17 patients. In addition to the typical findings of hepatocellular carcinomas (HCCs), such as arterial phase hyperenhancement (APHE), wash out, restricted diffusion, capsule and non-uptake at the hepatobiliary phase (HBP), the most common findings in MTM-HCCs were necrosis in 11 patients (64.7%, 11/17), followed by intratumoral arteries in 6 patients (35.3%, 6/17), peritumoral arterial transitive enhancement in 3 patients (17.6%, 3/17) and peritumoral hypointensive areas at the HBP in 3 of 8 patients (37.5%, 3/8) who received gadolinium-ethoxybenzyl-diethylenetriamine penta-acetic acid (Gd-EOB-DTPA) enhancement. The tumor size of non-MTM-HCCs was  $5.26 \pm 1.94$  cm, which was smaller than the  $8.58 \pm 2.83$  cm of MTM-HCCs ( $P < 0.001$ ). The frequency of necrosis and intratumoral arteries was significantly higher in MTM-HCCs than in non-MTM-HCCs (necrosis: 64.7% vs. 34.6%,  $P = 0.012$ ; intratumoral arteries: 47.1% vs. 19.7%,  $P = 0.008$ ).

**Conclusions:** MTM-HCCs tend to be large in size with intratumoral artery and intratumoral necrosis, which are characteristics that may distinguish them from non-MTM-HCCs.

**Keywords:** Computed tomography (CT); magnetic resonance imaging (MRI); hepatocellular carcinoma (HCC); macrotrabecular-massive

Submitted Sep 08, 2022. Accepted for publication Apr 28, 2023. Published online May 18, 2023.

doi: 10.21037/qims-22-940

View this article at: <https://dx.doi.org/10.21037/qims-22-940>

## Introduction

Hepatocellular carcinoma (HCC) is currently the sixth most common cancer and the third most common primary cause of cancer mortality worldwide (1). Similar to other kinds of cancers, HCC is heterogeneous and develops and evolves from various genetic or molecular profiles. Different pathologic and molecular phenotypes of HCC show different biological behaviors. Due to the greater understanding of its genetic and molecular profiles, the histopathologic category of HCCs has recently been modified substantially. According to the 2019 5<sup>th</sup> edition of the World Health Organization (WHO) classification, 65% of all HCCs are classified as not-otherwise-specified HCCs (NOS-HCCs), which have no distinguishing histopathologic features, and the remaining HCCs are classified into the following eight subtypes: steatohepatic, clear cell, macrotrabecular-massive (MTM), scirrhous, chromophobe, fibrolamellar, neutrophil-rich, and lymphocyte-rich (2). Among these HCC variants, the MTM subtype is associated with angiogenesis activation and worse prognosis (3,4). Therefore, distinguishing MTM-HCCs from other subtypes is necessary for predicting prognosis and making treatment decisions for patients with HCCs in the era of precision medicine.

Imaging plays a pivotal role in the diagnosis of HCCs, providing a definitive diagnosis on the basis of the typical characteristics of arterial phase hyperenhancement (APHE) and washout at the portal vein phase. Due to their unique histopathological characteristics, some HCC subtypes do not manifest the classic imaging features, which creates diagnostic challenges but also raises the suggestion of certain HCC variants. Familiarity with these imaging features might be helpful for establishing a diagnosis of HCC and suggesting certain subtypes. The purpose of this study was to describe the CT and MRI findings of MTM-HCCs and compare them with histopathological features. We present this article in accordance with the STROBE reporting checklist (available at <https://qims.amegroups.com/article/view/10.21037/qims-22-940/rc>).

## Methods

### Patients

This study was conducted in accordance with the Declaration of Helsinki (as revised in 2013). The study was approved by the institutional review board of Shenzhen People's Hospital, and individual consent for this retrospective case-control study was waived. We searched the pathological database of Shenzhen People's Hospital from January 2018 to June 2022. In our institution, the classification of MTM-HCC was not adopted prior to January 2018. Twenty-three consecutive patients with MTM-HCCs were identified from a total of 304 patients with HCCs, with a prevalence of 7.6%. The inclusion criteria were as follows: (I) CT or MRI performed within three months before surgery; (II) no antitumor therapy before surgery; and (III) a mass larger than 1 cm with good image quality. Seventeen eligible patients with MTM-HCCs were included after excluding 2 patients with an interval between CT or MRI imaging and surgery of more than 3 months and 4 patients due to receiving antitumor therapy. The final patient group consisted of 11 males and 6 females with an age of  $52.9 \pm 14.7$  years. To compare the most common findings of MTM-HCCs with those of non-MTM-HCCs, 232 patients fulfilling the inclusion criteria from among the 281 patients with non-MTM-HCCs were additionally included as the control group. The 232 patients consisted of 145 males and 87 females with an age of  $57.1 \pm 12.8$  years. The patient selection flow chart is shown in *Figure 1*. Fifty-nine patients underwent both CT and MRI, 35 underwent MRI only, and 138 underwent CT only. The differences in age and sex distribution between patients with non-MTM-HCCs and patients with MTM-HCCs were not statistically significant.

### CT and MRI examination

Among the 17 patients, 5 patients underwent only CT examination, 3 patients underwent only MRI examination,

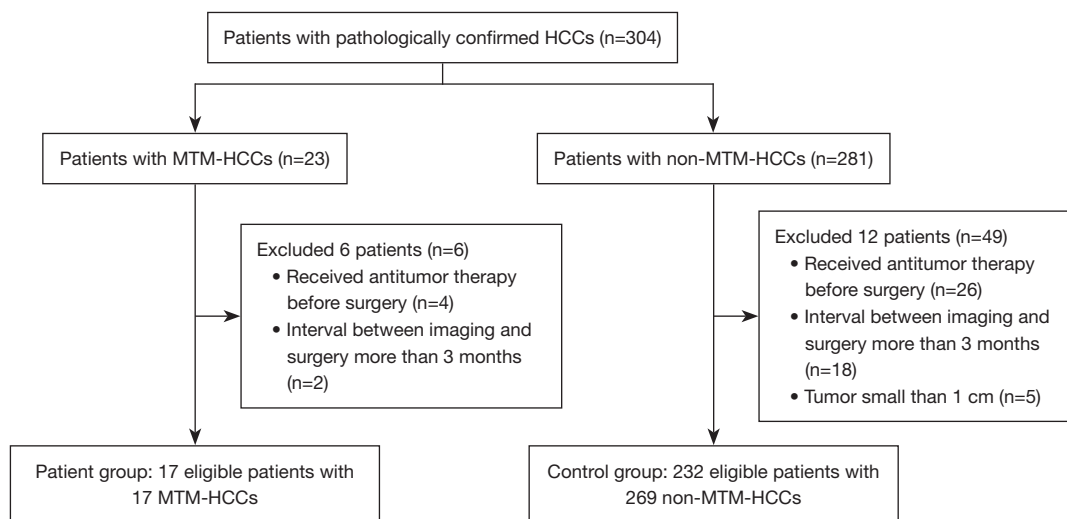


**Figure 1** Patient selection flowchart. HCCs, hepatocellular carcinomas; MTM-HCCs, macrotrabecular massive hepatocellular carcinomas.

and 9 patients underwent both CT and MRI examinations. All CT examinations were performed with a 128-row CT unit (Brilliance iCT, Philips Healthcare, Best, the Netherlands), and all MRI examinations were performed using a 3-T MRI system (Magnetom Skyra; Siemens Healthcare, Erlangen, Germany) or a 1.5-T MRI system (Multiva; Philips Healthcare). The dynamic enhanced CT examination protocol was performed as follows: after unenhanced scanning, 100 mL of nonionic iodinated contrast material was injected at a rate of 3–4 mL/s followed by 20 mL of 0.9% saline; arterial phase scanning was performed at 30 s after the initial injection, portal vein phase scanning at 70 s, and delayed phase scanning at 180 s. For MRI examinations, after pre-contrast images [breath-hold fat-suppressed turbo spin-echo T2-weighted sequence, breath-hold out-of-phase and in-phase T1-weighted sequences, and diffusion-weighted imaging (DWI) with two b values (0 and 800 s/mm<sup>2</sup>)], dynamic contrast-enhanced images were obtained by intravenous injection of 0.1 mmol/kg gadopentetate dimeglumine (Gd-DTPA) (Magnevist; Beijing Beilu Pharmaceutical Co., Ltd., Beijing, China) in 4 patients or 0.025 mmol/kg gadoxetic acid disodium [gadolinium-ethoxybenzyl-diethylenetriamine penta-acetic acid (Gd-EOB-DTPA)] (Primovist, Bayer Schering, Berlin, Germany) in 8 patients at a rate of 2 mL/s followed by 20 mL of 0.9% saline flush using the breath-hold out-of-phase T1-weighted sequence. Arterial phase, portal phase and delayed phase images were acquired at a delay of 25 and 70 s after the initial injection. For Gd-EOB-DTPA enhancement, hepatobiliary phase (HBP) acquisition

was performed 20 min after contrast administration. The apparent diffusion coefficient (ADC) was automatically calculated by the MRI system based on the two b values of DWI.

### Image analysis

Two radiologists with more than 5 years of experience in abdominal imaging interpretation independently reviewed the CT and MRI images. Although they were aware of the diagnosis of HCC, they did not know the subtypes of the tumors and reviewed both MTM-HCCs and non-MTM-HCCs randomly. Any disagreement among the readers was resolved by consulting another radiologist with 10 years of experience in abdominal imaging interpretation who was blinded to the tumor subtype.

### Statistical analysis

The chi-square test or Fisher's exact test was used for categorical data, and Student's *t*-test or the Mann-Whitney U test was used for continuous variables to compare the difference between imaging manifestations of MTM-HCCs and non-MTM-HCCs as appropriate. All statistical tests were two-tailed, and P values <0.05 were considered statistically significant.

## Results

Seventeen tumors, which measured 8.58±2.83 cm at the

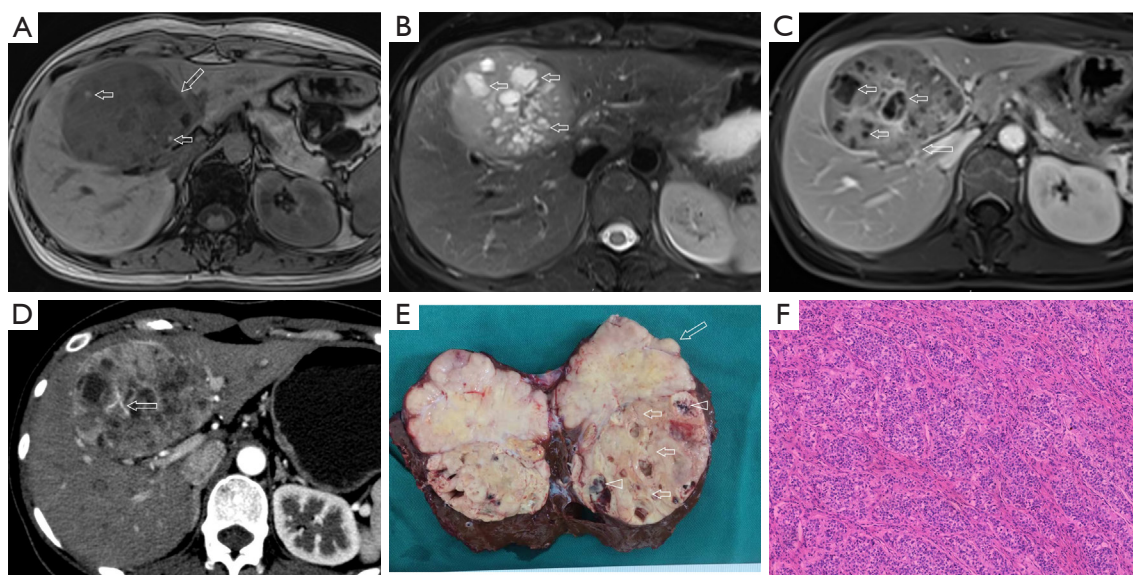


**Figure 2** A 28-year-old woman with MTM-HCC. (A) Transversal non-contrast-enhanced T1-weighted MR image with fat suppression shows a heterogeneous 90-mm mass with hyperintense foci (short arrows), which might be hemorrhage, and hypointense areas (long arrows). (B) Transversal non-contrast-enhanced T2-weighted MR image with fat suppression shows multiple hyperintense areas (arrows), which is consistent with necrosis. (C) Contrast-enhanced T1-weighted MR image with fat suppression shows heterogeneity enhancement with multiple hypointense necrosis areas (short arrows). The margin of the tumor is irregular with a lobulated bulge (long arrow). (D) Transversal contrast-enhanced CT image at the arterial phase shows heterogeneity enhancement with intratumoral arteries (arrow). (E) Photograph of the gross pathologic specimen shows a lobulated margin mass (long arrow) with hemorrhagic foci (arrowheads) and necrotic areas (short arrows). (F) Microscopic examination (hematoxylin-eosin stain,  $\times 100$ ) shows a thick trabecular formation surrounded by vascular spaces, which is consistent with the diagnosis of MTM-HCC. MR, magnetic resonance; CT, computed tomography; MTM-HCC, macrotrabecular massive hepatocellular carcinoma.

maximum transverse section, were resected from 17 patients. The most common finding in MTM-HCCs was necrosis in 11 patients (64.7%), followed by intratumoral arteries in 8 patients (47.1%). Representative CT and magnetic resonance (MR) images with pathological correlations are shown in *Figures 2,3*. Intratumoral necrosis could be a large central irregular area (*Figure 4*) or multiple small areas. Necrotic areas were identified at gross pathologic examination (*Figures 2E,3E*). In one patient, intratumoral hemorrhage appeared as active contrast material leak (*Figure 5*). The tumor margins were not smooth in 6 cases (35.3%). Peritumoral arterial transitive enhancement was found in 3 patients (17.6%) and peritumoral HBP hypointensity in 3 of 8 patients (37.5%) who received Gd-EOB-DTPA enhancement (*Figure 6*). Microvascular invasiveness (MVI) was observed in the tumors with peritumoral HBP hypointensity. Satellite nodules were identified in only one patient (5.9%) (*Figure 3*). In the 232 patients with non-MTM-HCCs, 269 masses were

detected and resected, with 37 patients having 2 masses; the masses measured  $5.26 \pm 1.94$  cm, which was smaller than the  $8.58 \pm 2.83$  cm of MTM-HCCs ( $P < 0.001$ ). The occurrence rates of necrosis and intratumoral arteries were 64.7% and 47.1%, respectively, in MTM-HCCs and 34.6% and 19.7%, respectively, in non-MTM-HCCs, which was a statistically significant difference, while the difference in non-smooth margins (35.3% *vs.* 26.4%) was not statistically significant (*Table 1*). In addition, the occurrence rates of typical HCC findings, such as APHE and washout, were not significantly different between MTM-HCCs and non-MTM-HCCs.

## Discussion

MTM-HCC was identified as a novel histological subtype of HCC in 2017; it is associated with aggressive biological behavior and a worse prognosis. Due to its high rate of early and overall recurrence after surgical resection or radiofrequency ablation, distinguishing MTM-HCCs

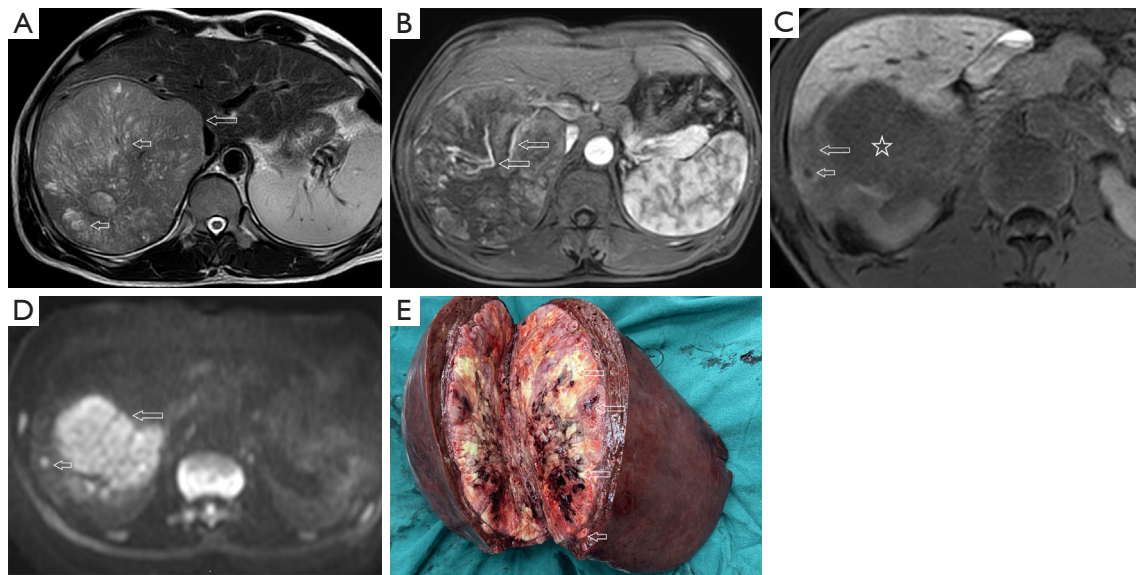


**Figure 3** A 52-year-old man with MTM-HCC. (A) Transversal non-contrast-enhanced T2-weighted MR image shows a lobulated mass (long arrow) with multiple hyperintense foci or strands (short arrows), indicating necrosis. (B) Transversal arterial phase T1-weighted MR image with fat suppression shows intratumoral arteries (arrows). (C) Transversal HBP T1-weighted MR image with fat suppression shows that a hypointense mass (star) and a satellite nodule (short arrow) within the peritumoral HBP hypointensity (long arrow). (D) Transversal diffusion-weighted MR image with a b value of 800 s/mm<sup>2</sup> shows restricted diffusion (long arrow) and a hyperintense satellite nodule (short arrow). (E) Photograph of the gross pathologic specimen shows strands and foci of necrosis and hemorrhage (long arrows) and a satellite nodule (short arrow). MTM-HCC, macrotrabecular massive hepatocellular carcinoma; MR, magnetic resonance; HBP, hepatobiliary phase.



**Figure 4** A 32-year-old man with MTM-HCC. Transversal portal phase CT image shows a large mass with peripheral enhancement and a large area of necrosis (star). MTM-HCC, macrotrabecular massive hepatocellular carcinoma; CT, computed tomography.

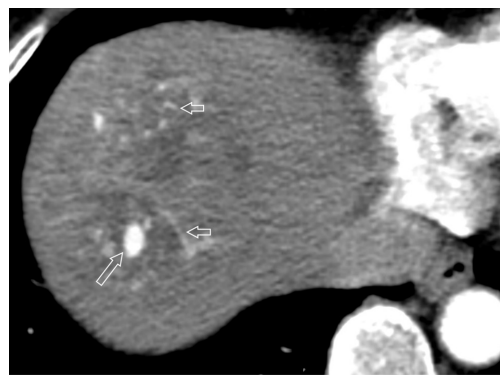


**Figure 5** A 65-year-old man with MTM-HCC. Transversal arterial phase CT image shows a focus of active contrast agency leak (long arrow), which is consistent with bleeding and intratumoral arteries (short arrows). MTM-HCC, macrotrabecular massive hepatocellular carcinoma; CT, computed tomography.

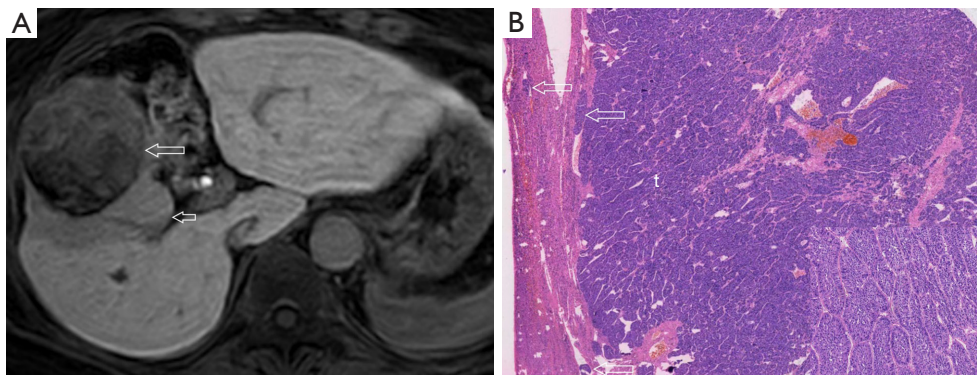


**Figure 6** A 67-year-old man with MTM-HCC. (A) Transversal HBP T1-weighted MR image with fat suppression shows that a hypointense mass (long arrow) and peritumoral HBP hypointensity (short arrow). (B) Microscopic examination (hematoxylin-eosin stain,  $\times 40$ ) shows tumor cells in a vessel (arrows) outside the main tumor (t), indicating MVI. The insert shows tumor cells with a predominant macrotrabecular pattern (hematoxylin-eosin stain,  $\times 100$ ). MTM-HCC, macrotrabecular-massive hepatocellular carcinoma; HBP, hepatobiliary phase; MR, magnetic resonance; MVI, microvascular invasiveness.

**Table 1** Comparison of the most common imaging findings of MTM-HCCs with non-MTM-HCCs

Variables	MTM-HCCs (n=17), n (%)	Non-MTM-HCCs (n=269), n (%)	P value
Necrosis	11 (64.7)	93 (34.6)	0.012
Intratumoral arteries	8 (47.1)	53 (19.7)	0.008
Non-smooth margins	6 (35.3)	71 (26.4)	0.422
APHE	13 (76.5)	173 (64.3)	0.308
Washout	11 (64.7)	159 (59.1)	0.649

APHE, arterial phase hyperenhancement; MTM-HCCs, macrotrabecular-massive hepatocellular carcinoma.

from other subtypes might pave the way for personalized medicine for patients with HCCs (3,4). Unlike other kinds of cancers, diagnosis of HCCs can be obtained by relying on classic imaging findings in most cases. Therefore, diagnosis of MTM-HCCs by noninvasive imaging could optimize treatment decision-making.

In this study, we reported the CT and MRI findings of 17 cases of pathologically confirmed MTM-HCCs. In addition to the conventional imaging findings of HCCs, the most common other findings of MTM-HCCs were intratumoral necrosis, followed by intratumoral arteries. Due to proliferation of tumor cells into layers 6 cells thick, increased cellularity and diffusion distance from the vascular supply might lead to hypoxia and prominent necrosis. Mulé *et al.* reported that necrosis and size were independent predictors for MTM-HCC (5). Substantial necrosis (involving at least 20% of the tumor) helped to identify 65% of MTM-HCCs with a specificity of 93% (6).

Necrosis could be a large central area or multiple diffuse small areas. Genetic profiling showed that MTM-HCCs had a strong association with hypoxia-related gene expression, which might be another driver of necrosis (7). The intratumoral arteries were related to angiogenesis, which was demonstrated by neoplastic cells arranged in thick trabeculae surrounded by abundant vascular spaces. Angiogenesis activation has been demonstrated to be a hallmark feature of MTM-HCCs (8). Although intratumoral hemorrhage was reported to be common in MTM-HCCs (5,6), active contrast agent leak was identified in one tumor in this series, which may have resulted from vascular invasiveness by tumor cells. Additional imaging characteristics included irregular tumor margins, peritumoral enhancement during the arterial phase and peritumoral HBP hypointensity, which were consistent with aggressiveness at pathological examinations. Both peritumoral enhancement during the arterial phase and

peritumoral hypointensity in the HBP have been reported to be associated with MVI in patients with HCCs (9-12). MVI is an important predictor of early recurrence after resection, overall survival, and posttransplant recurrence (13). Both radiological and pathological studies have reported that satellite nodules are associated with MTM-HCCs (3,6-8,14,15). Satellite nodules were only identified in one patient in this study. At our institute, if the tumor had satellite nodules, patients often received palliative therapy or bridge treatment before surgical resection. Therefore, satellite nodules might be a common finding of MTM-HCCs, but tumors with satellite nodules may have been excluded in this retrospective series. To compare the most common findings of MTM-HCCs, 232 patients with 269 non-MTM-HCCs were recruited. The tumor size of MTM-HCCs tended to be larger than that of non-MTM-HCCs. Among the three most common findings of MTM-HCCs, in addition to the conventional imaging findings of HCCs, the occurrence rates of necrosis and intratumoral arteries were significantly higher than those of non-MTM-HCCs. These findings were consistent with the literature and were considered imaging characteristics of MTM-HCCs to distinguish them from non-MTM-HCCs (3,5,6,9). Although the prevalence of non-smooth margins of MTM-HCCs was high in this series, the difference between the two groups was not statistically significant.

This study has several limitations. First, only imaging findings of resected MTM-HCCs were included. Therefore, the selection bias might preclude some imaging characteristics of the MTM-HCCs that did not undergo surgery, such as satellite nodules. Second, imaging findings were not encoded into the Liver Imaging Reporting and Data System (LI-RADS). Third, it has been reported in the literature that intratumoral necrosis might result from hypoxia. Due to the retrospective nature of this study, the hypoxia status of MTM-HCCs was not investigated. Finally, because only 35% of all HCCs can be classified into eight subtypes, imaging findings of MTM-HCCs were not compared with other types of HCCs in this small group series.

## Conclusions

In addition to the conventional findings of HCCs, MTM-HCCs are more likely to be of large size with intratumoral arteries and multiple small areas of necrosis or a large central necrosis. Peritumoral arterial phase enhancement and HBP hypointensity can sometimes be observed.

These imaging characteristics are associated with the histopathological features of MTM-HCCs. Familiarity with these imaging features may facilitate radiologists to suggest the possibility of MTM-HCCs, which would be helpful for personalized patient treatment decision-making.

## Acknowledgments

*Funding:* None.

## Footnote

*Reporting Checklist:* The authors have completed the STROBE reporting checklist. Available at <https://qims.amegroups.com/article/view/10.21037/qims-22-940/rc>

*Conflicts of Interest:* All authors have completed the ICMJE uniform disclosure form (available at <https://qims.amegroups.com/article/view/10.21037/qims-22-940/coif>). The authors have no conflicts of interest to declare.

*Ethical Statement:* The authors are accountable for all aspects of the work in ensuring that questions related to the accuracy or integrity of any part of the work are appropriately investigated and resolved. This study was conducted in accordance with the Declaration of Helsinki (as revised in 2013). The study was approved by the institutional review board of Shenzhen People's Hospital, and individual consent for this retrospective analysis was waived.

*Open Access Statement:* This is an Open Access article distributed in accordance with the Creative Commons Attribution-NonCommercial-NoDerivs 4.0 International License (CC BY-NC-ND 4.0), which permits the non-commercial replication and distribution of the article with the strict proviso that no changes or edits are made and the original work is properly cited (including links to both the formal publication through the relevant DOI and the license). See: <https://creativecommons.org/licenses/by-nc-nd/4.0/>.

## References

1. Sung H, Ferlay J, Siegel RL, Laversanne M, Soerjomataram I, Jemal A, Bray F. Global Cancer Statistics 2020: GLOBOCAN Estimates of Incidence and Mortality Worldwide for 36 Cancers in 185 Countries. *CA Cancer J Clin* 2021;71:209-49.

2. Loy LM, Low HM, Choi JY, Rhee H, Wong CF, Tan CH. Variant Hepatocellular Carcinoma Subtypes According to the 2019 WHO Classification: An Imaging-Focused Review. *AJR Am J Roentgenol* 2022;219:212-23.
3. Ziol M, Poté N, Amaddeo G, Laurent A, Nault JC, Oberti F, et al. Macrotrabecular-massive hepatocellular carcinoma: A distinctive histological subtype with clinical relevance. *Hepatology* 2018;68:103-12.
4. Yoon JH, Kim H. CT Characterization of Aggressive Macrotrabecular-Massive Hepatocellular Carcinoma: A Step Forward to Personalized Medicine. *Radiology* 2021;300:230-2.
5. Mulé S, Serhal A, Pregliasco AG, Nguyen J, Vendrami CL, Reizine E, Yang GY, Calderaro J, Amaddeo G, Luciani A, Miller FH. MRI features associated with HCC histologic subtypes: a western American and European bicenter study. *Eur Radiol* 2023;33:1342-52.
6. Mulé S, Galletto Pregliasco A, Tenenhaus A, Kharrat R, Amaddeo G, Baranes L, Laurent A, Regnault H, Sommacale D, Djabbari M, Pigneur F, Tacher V, Kobeiter H, Calderaro J, Luciani A. Multiphase Liver MRI for Identifying the Macrotrabecular-Massive Subtype of Hepatocellular Carcinoma. *Radiology* 2020;295:562-71.
7. Calderaro J, Meunier L, Nguyen CT, Boubaya M, Caruso S, Luciani A, et al. ESM1 as a Marker of Macrotrabecular-Massive Hepatocellular Carcinoma. *Clin Cancer Res* 2019;25:5859-65.
8. Calderaro J, Couchy G, Imbeaud S, Amaddeo G, Letouzé E, Blanc JF, Laurent C, Hajji Y, Azoulay D, Bioulac-Sage P, Nault JC, Zucman-Rossi J. Histological subtypes of hepatocellular carcinoma are related to gene mutations and molecular tumour classification. *J Hepatol* 2017;67:727-38.
9. Zhang L, Yu X, Wei W, Pan X, Lu L, Xia J, Zheng W, Jia N, Huo L. Prediction of HCC microvascular invasion with gadobenate-enhanced MRI: correlation with pathology. *Eur Radiol* 2020;30:5327-36.
10. Dong SY, Wang WT, Chen XS, Yang YT, Zhu S, Zeng MS, Rao SX. Microvascular invasion of small hepatocellular carcinoma can be preoperatively predicted by the 3D quantification of MRI. *Eur Radiol* 2022;32:4198-209.
11. Lei Z, Li J, Wu D, Xia Y, Wang Q, Si A, Wang K, Wan X, Lau WY, Wu M, Shen F. Nomogram for Preoperative Estimation of Microvascular Invasion Risk in Hepatitis B Virus-Related Hepatocellular Carcinoma Within the Milan Criteria. *JAMA Surg* 2016;151:356-63.
12. Kim KA, Kim MJ, Jeon HM, Kim KS, Choi JS, Ahn SH, Cha SJ, Chung YE. Prediction of microvascular invasion of hepatocellular carcinoma: usefulness of peritumoral hypointensity seen on gadoxetate disodium-enhanced hepatobiliary phase images. *J Magn Reson Imaging* 2012;35:629-34.
13. Sumie S, Nakashima O, Okuda K, Kuromatsu R, Kawaguchi A, Nakano M, Satani M, Yamada S, Okamura S, Hori M, Kakuma T, Torimura T, Sata M. The significance of classifying microvascular invasion in patients with hepatocellular carcinoma. *Ann Surg Oncol* 2014;21:1002-9.
14. Yoon JK, Choi JY, Rhee H, Park YN. MRI features of histologic subtypes of hepatocellular carcinoma: correlation with histologic, genetic, and molecular biologic classification. *Eur Radiol* 2022;32:5119-33.
15. Rhee H, Cho ES, Nahm JH, Jang M, Chung YE, Baek SE, Lee S, Kim MJ, Park MS, Han DH, Choi JY, Park YN. Gadoteric acid-enhanced MRI of macrotrabecular-massive hepatocellular carcinoma and its prognostic implications. *J Hepatol* 2021;74:109-21.

**Cite this article as:** Gong Q, Zhang Y, Wu T, Du Z, Zhang Y. Comparison of computed tomography and magnetic resonance imaging findings and histopathological features of macrotrabecular-massive hepatocellular carcinoma. *Quant Imaging Med Surg* 2023;13(7):4633-4640. doi: 10.21037/qims-22-940